

Research article

Comparison of Interferometry Applications: Michelson vs. Sagnac Interferometers

Thanawat Wannasri, Witoon Yindeesuk* and Prathan Buranasiri

*Department of Physics, School of Science, King Mongkut's Institute of Technology
Ladkrabang, Bangkok, Thailand*

Received: 10 July 2024, Revised 15 November 2024, Accepted: 20 November 2024, Published: 11 March 2025

Abstract

An interferometer is a crucial instrument for collecting information on interference patterns, widely used in both scientific and industrial applications. This paper was focused on comparing the interferometric applications of the Michelson and Sagnac interferometers. The Michelson interferometer, characterized by its double-path setup, and the Sagnac interferometer, which operates on a common-path principle, were analyzed. Experiments were conducted to capture interference patterns of different samples using both interferometers. In the first experiment, the image fringes of the alphabet characters (K, M, I, T, and L) were captured, while in the second, fingerprint patterns were captured. The results showed that both interferometers produced similar fringes for the alphabet characters, although the Sagnac interferometer exhibited a higher circular frequency. In the fingerprint experiment, the Michelson interferometer produced linear fringes. This study highlights the distinct fringe patterns generated by each interferometer when different samples are analyzed, providing valuable insights into their diverse applications.

Keywords: interference patterns; Michelson interferometer; Sagnac interferometer; fringe analysis; optical paths

1. Introduction

Interferometry, a cornerstone in precision measurement and scientific exploration, is exemplified by two widely utilized interferometers- the Michelson and Sagnac. Each of these devices boasts unique capabilities and applications, making them invaluable in various fields of research and industry (Malacara & Harris, 1970; Shaddock et al., 1998; Yu et al., 2024).

The Michelson interferometer, invented by Albert A. Michelson, is renowned for its applications in the measurement of wavelengths and refractive indices, and for its pivotal role in the Michelson-Morley experiment, which provided critical evidence for the theory of relativity (Ferrari et al., 2002; Schnars & Jueptner, 2005). The setup of the Michelson interferometer, as illustrated in Figure 1, splits a beam of light into two paths using a beam splitter. These paths are reflected by mirrors and then recombined to produce interference patterns, which are analyzed to determine precise measurements of distances and changes in optical paths (Usman et al., 2024).

*Corresponding author: E-mail: witoon.yi@kmitl.ac.th
<https://doi.org/10.55003/cast.2025.263978>

Copyright © 2024 by King Mongkut's Institute of Technology Ladkrabang, Thailand. This is an open access article under the CC BY-NC-ND license (<http://creativecommons.org/licenses/by-nc-nd/4.0/>).

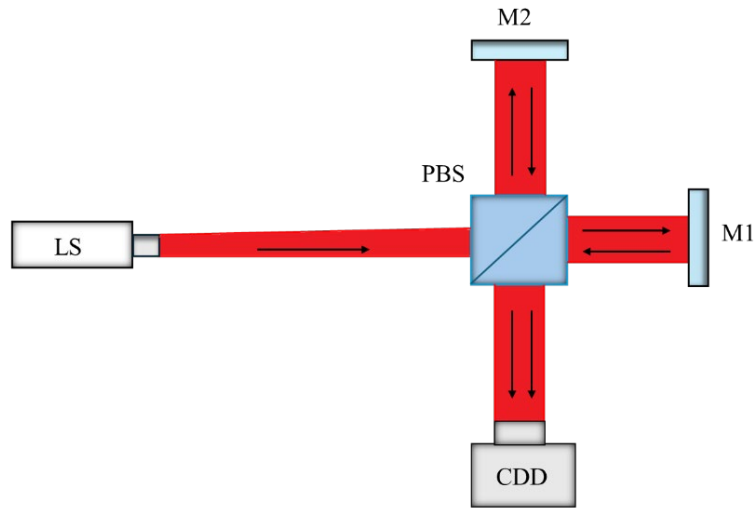


Figure 1. Experimental setup of the Michelson interferometer

In contrast, the Sagnac interferometer, introduced by Georges Sagnac, features a fundamentally different configuration and application. It is particularly sensitive to rotational motion, making it essential in gyroscope technologies for navigation and geophysics (Usman et al., 2021). As shown in Figure 2, the Sagnac interferometer splits light into two beams traveling in opposite directions around a loop. The interference pattern formed by the recombined beams shifts when the device rotates, allowing for the measurement of angular velocity with high precision (Joel Nathan et al., 2018; Usman et al., 2022).

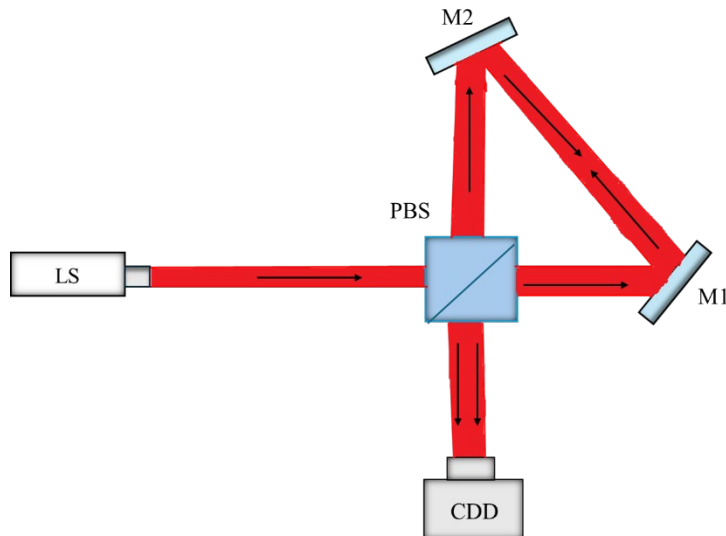


Figure 2. Experimental setup of the Sagnac interferometer

Recent advancements have further extended the capabilities of these interferometers. For instance, the Michelson interferometer with Bessel beams has enhanced propagation-invariance and self-healing properties, making it suitable for high-precision measurements in complex environments (Yu et al., 2024). Studies have shown that the Sagnac interferometer, when combined with advanced phase shift techniques, exhibits superior noise tolerance and environmental robustness compared to the Mach-Zehnder interferometer (Xiao et al., 2018).

Moreover, the development of modified Sagnac interferometers using circularly polarized light and phase shift techniques has shown significant improvements in the measurement of transparent thin-film thicknesses and nanoscale tilt measurements. These advancements illustrate the potential of both interferometers in expanding their applications beyond traditional uses, providing more robust and precise measurements in various scientific and engineering fields.

This study was aimed at providing a comparative analysis of the Michelson and Sagnac interferometers by examining their interference patterns under various experimental conditions. By analyzing the distinct fringe patterns produced by each interferometer, we sought to highlight their respective advantages and practical applications. This comparative study can contribute to a deeper understanding of the optimal conditions and contexts for employing each type of interferometer, thereby enhancing their practical applications in scientific research and industry.

The Michelson interferometer uses a beam splitter to divide a beam of light into two perpendicular arms, each with a mirror. The light reflects off these mirrors and then recombines at the beam splitter to produce interference. The resulting fringe pattern depends on the difference in optical path length between the two arms, typically resulting in circular or concentric fringes:

$$\Delta L = m\lambda \quad (1)$$

where:

ΔL is the difference in distance traveled by the light in the two arms,
 m is the number of fringes shifted,
 λ is the wavelength of light.

The Sagnac interferometer operates in a loop configuration. Light is split into two beams traveling in opposite directions around a loop, which then recombine and interfere. The interference pattern depends on the relative motion between the light paths due to rotation, leading to linear fringe shifts or displacement rather than concentric patterns:

$$\Delta\phi = \frac{8\pi A \cdot \Omega}{\lambda_c} \quad (2)$$

where:

$\Delta\phi$ is the phase difference,
 A is the area enclosed by the light path,
 Ω is the angular velocity of rotation,
 λ_c is the wavelength of light.

In both the Michelson and Sagnac interferometers, the phase difference plays a crucial role in the formation of fringes. Fringe patterns arise due to constructive or destructive interference of light beams with different phase differences. Constructive

interference leads to bright fringes, while destructive interference leads to dark fringes. Any change in the phase difference, whether from a shift in the light path length or rotation of the interferometer, alters the fringe position:

$$\Delta\phi = \frac{2\pi\Delta L}{\lambda_c} \quad (3)$$

where ΔL is the difference in path length traveled by the light, and λ_c is the wavelength of light.

These equations help explain the distinctive fringe patterns produced by each interferometer. The Michelson interferometer's setup results in precise circular fringes, while the Sagnac interferometer's sensitivity to rotation leads to linear fringe shifts.

2. Materials and Methods

2.1 Recording the image fringes of the alphabet

Figures 3 and 4 illustrate the experimental setup for capturing the image fringes of alphabet samples (K, M, I, T, and L) using the Michelson and Sagnac interferometers. Each character of the alphabet samples was mounted on a transparent glass slide, with each character having a height of 4.6 mm and a width of 5.5 mm. This size was selected to provide a well-defined structure for observing the circular fringes characteristic of the Michelson interferometer and the higher frequency fringes of the Sagnac interferometer.

The Michelson interferometer setup (Figure 3) employed a semiconductor laser with a wavelength of 632.8 nm as the light source. A convex lens focused at 15 cm was used to enhance the visibility of the fringes. The beam splitter divided the light beam into two paths, which were then reflected by two mirrors to create interference patterns. These patterns were captured using a CCD camera (Canon EOS 700D). The camera was set at an ISO of 100 with an exposure time of 1/200 s to capture high-contrast images, ensuring detailed fringe visibility. The camera resolution was 5184×2912 pixels (24-bit depth), with sRGB color representation.

The Sagnac interferometer setup (Figure 4) was similar but with the mirror angled at 20 degrees. The light beam was split into two beams traveling in opposite directions along a loop path. The interferometer produced fringes with higher circular frequency due to its configuration. The CCD camera settings remained the same as in the Michelson setup to maintain consistency in image acquisition.

2.2 Recording the image fringes of fingerprints

Figures 5 and 6 show the setups for capturing fingerprint image fringes using the Michelson and Sagnac interferometers. The fingerprint samples were chosen for their intricate swirl patterns, which consist of ridge and valley structures, providing complex and challenging details for the analysis of fringe patterns. Each fingerprint was etched onto a glass slide, with an approximate area of 10 mm x 10 mm, ensuring sufficient sample size for fringe observation.

The Michelson interferometer setup (Figure 5) used the same semiconductor laser (632.8 nm wavelength) and a convex lens to focus the beam at 15 cm, producing clear interference fringes. The CCD camera settings mirrored those of the alphabet experiment, capturing the fine details of the fingerprint fringes.

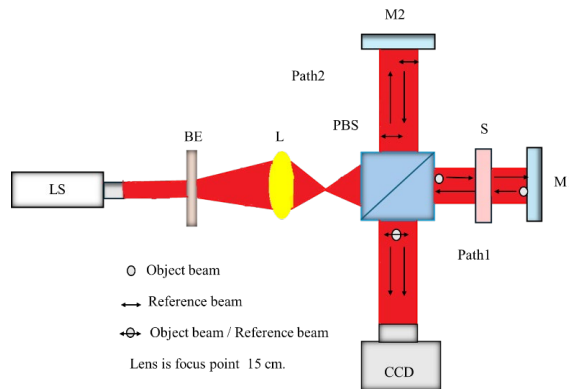
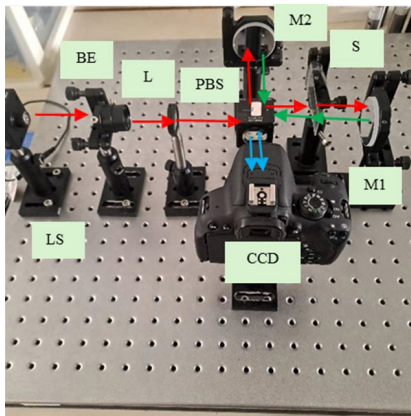


Figure 3. Experimental setup of the Michelson interferometer for capturing alphabet samples

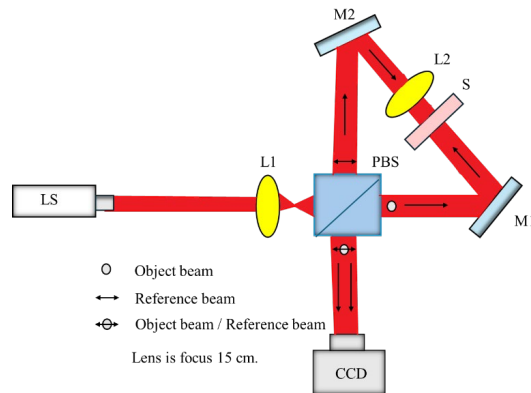
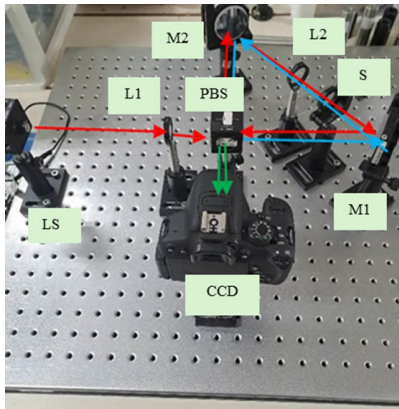


Figure 4. Experimental setup of the Sagnac interferometer for capturing alphabet samples

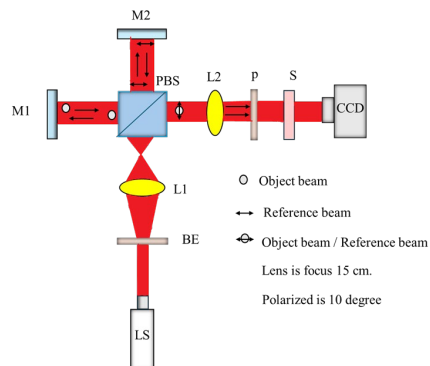
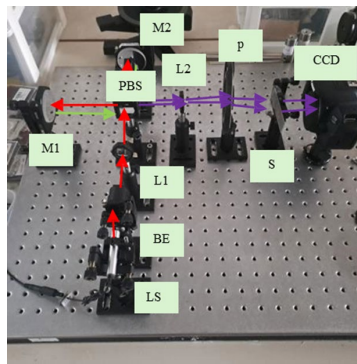


Figure 5. Experimental setup of the Michelson interferometer for capturing fingerprint samples

In the Sagnac interferometer setup (Figure 6), the light beam was similarly split and traveled in opposite directions around a loop. The camera's position and settings were optimized to capture the distinct linear fringes produced by the Sagnac interferometer's configuration.

By using these samples, the study compares the abilities of both interferometers to handle different fringe structures. The alphabet samples, with their regular shapes, allow for clear observation of interference patterns, while the fingerprints' complexity challenges the resolution and sensitivity of the interferometers, providing a comprehensive comparison.

This comprehensive setup and sample choice ensure a clear demonstration of the fringe patterns produced by both the Michelson and Sagnac interferometers.

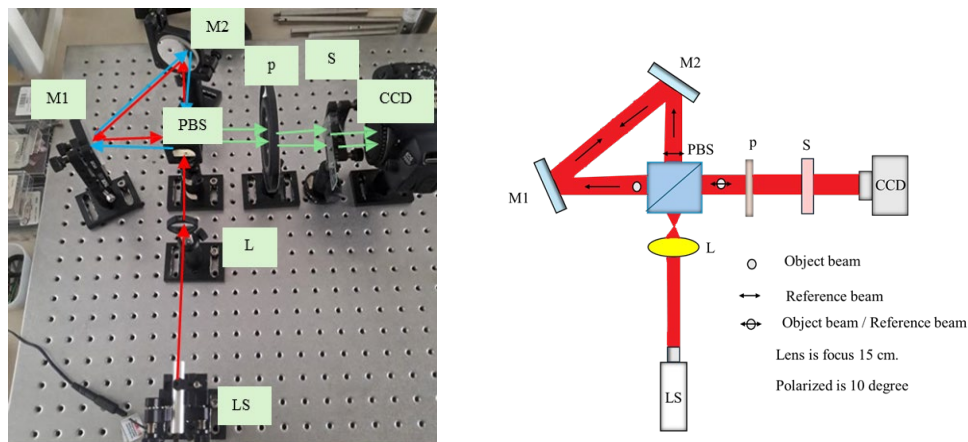


Figure 6. Experimental setup of the Sagnac interferometer for capturing fingerprint samples

4. Results and Discussion

4.1 Results: Alphabet (K, M, I, T, and L)

Figures 7 and 8 show the recorded image fringes of the alphabet character samples (K, M, I, T, and L) using the Michelson and Sagnac interferometers, respectively. For the Michelson interferometer, the fringes observed were circular, consistent with the expected output due to the interference of two coherent light beams that were split and recombined. The Sagnac interferometer, on the other hand, produced fringes with a higher circular frequency. This difference in fringe patterns highlights the unique capabilities of each interferometer. The Michelson interferometer is suitable for applications that require circular fringes, while the Sagnac interferometer's higher circular frequency makes it more suitable for other applications. These results provide valuable insights into the diverse applications of these interferometers.

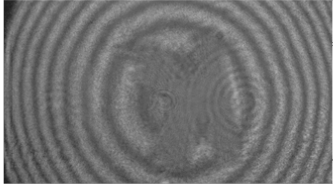
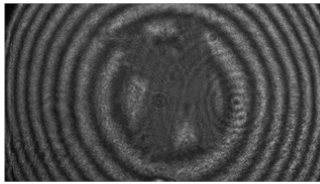
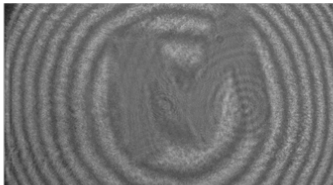
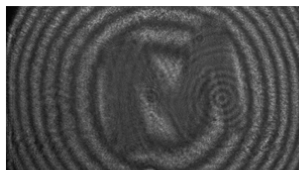
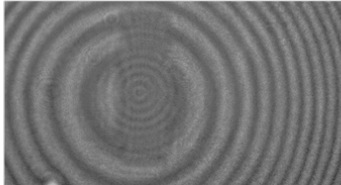
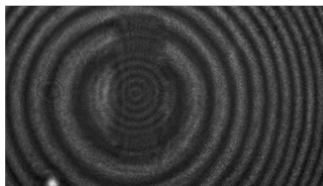
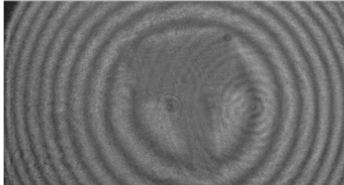
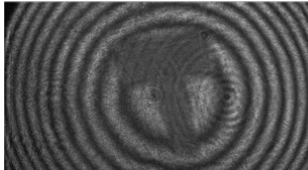
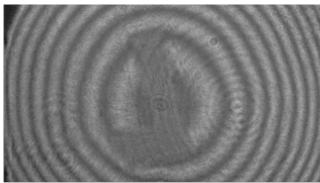
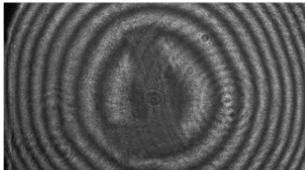
Alphabet image	Reconstruction Alphabet image
 Alphabet K (remove convex lens)	 Reconstruction Alphabet K
 Alphabet M (remove convex lens)	 Reconstruction Alphabet M
 Alphabet I (remove convex lens)	 Reconstruction Alphabet I
 Alphabet T (remove convex lens)	 Reconstruction Alphabet T
 Alphabet L (remove convex lens)	 Reconstruction Alphabet L

Figure 7. Interference fringes of alphabet character samples captured using michelson interferometer

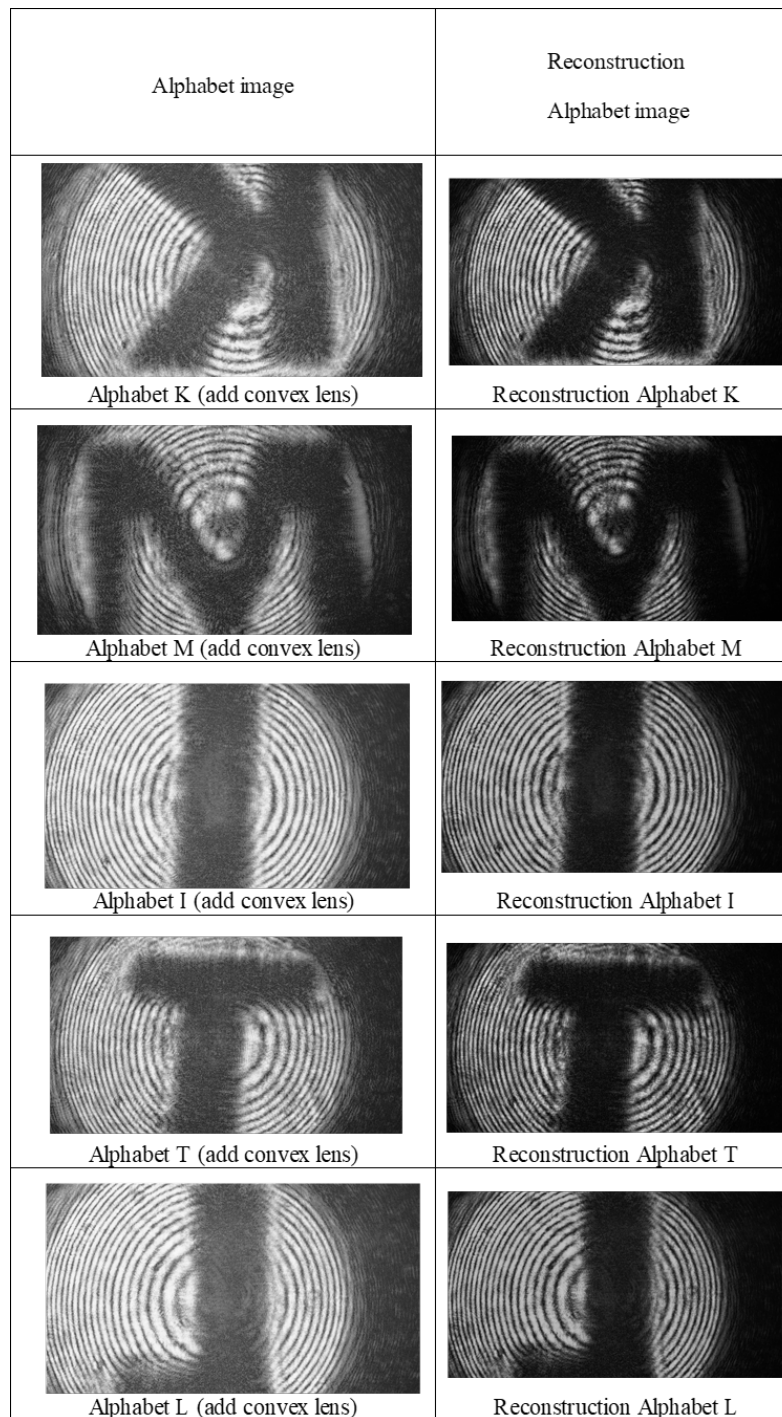


Figure 8. Interference fringes of alphabet character samples captured using sagnac interferometer

4.2 Results: Fingerprints

Figures 9 and 10 depict the recorded image fringes of fingerprints using the Michelson and Sagnac interferometers. For the Michelson interferometer, the fingerprint fringes appeared as concentric circles. This result aligns with the Michelson interferometer's ability to produce precise, circular interference patterns for various samples. The Sagnac interferometer, however, produced linear fringes. Removing the convex lens between the mirrors created diagonal fringes, which differ significantly from the Michelson's output. This demonstrates the Sagnac interferometer's unique ability to alter fringe patterns based on its optical setup.

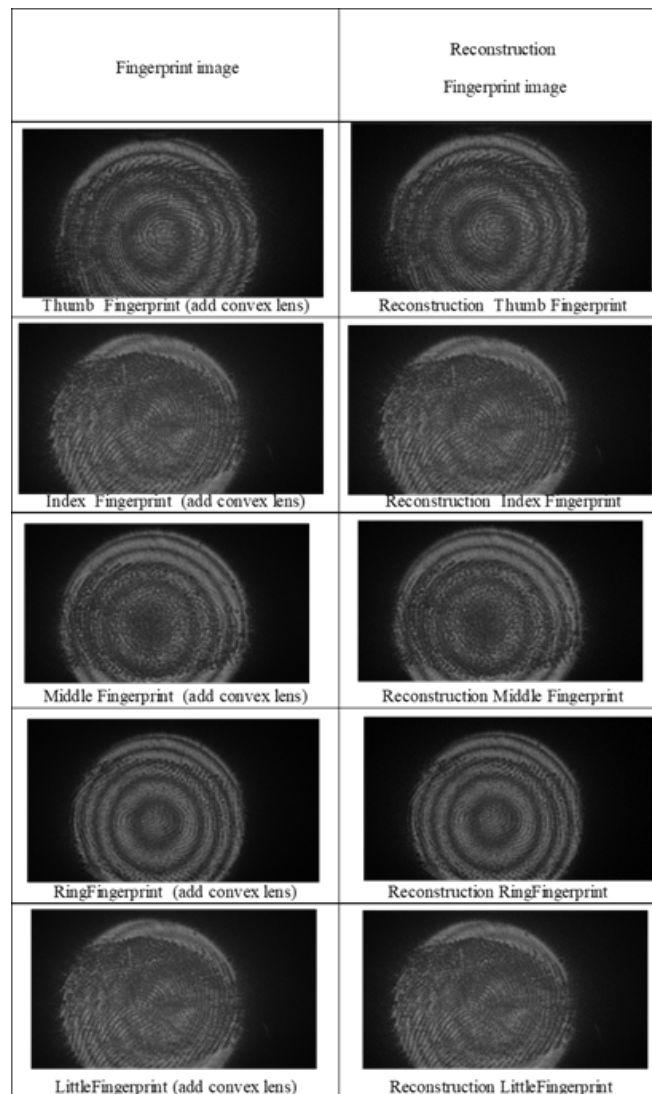


Figure 9. Interference fringes of fingerprint samples captured using Michelson interferometer



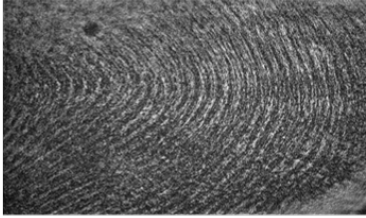
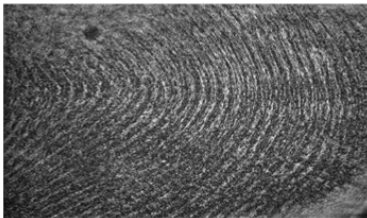






Fingerprint image	Reconstruction Fingerprint image
	
Thumb Fingerprint (remove convex lens)	Reconstruction Thumb Fingerprint
	
Index Fingerprint (remove convex lens)	Reconstruction Index Fingerprint
	
Middle Fingerprint (remove convex lens)	Reconstruction Middle Fingerprint
	
RingFingerprint (remove convex lens)	Reconstruction RingFingerprint
	
LittleFingerprint (remove convex lens)	Reconstruction LittleFingerprint

Figure 10. Interference fringes of fingerprint samples captured using Sagnac interferometer

4.3 Comparison of Michelson and Sagnac interferometers

The key characteristics of the Michelson and Sagnac interferometers, including their fringe patterns, fringe shifts, and applications, are summarized in Table 1. The Michelson interferometer primarily produces circular fringes and is sensitive to changes in optical path length, making it suitable for high-precision measurements. The Sagnac interferometer, in contrast, demonstrates a higher sensitivity to rotational motion and phase differences, resulting in fringe shifts that are useful in navigation and geophysics.

Table 1. Comparison of characteristics between Sagnac and Michelson interferometers

Characteristic	Sagnac Interferometer	Michelson Interferometer
Fringe pattern	Appears as straight lines or curves depending on the interferometer's rotation or path direction.	Appears as concentric rings or straight lines due to interference from perpendicular light paths.
Fringe shift due to external factors	A noticeable shift in fringe patterns occurs during rotation of the interferometer.	Fringe shifts occur when there is a change in the optical path length between the two beams.
Observed fringe behavior	During rotation, fringes shift due to phase differences between the two opposing light paths, indicating rotational motion.	Fringes shift forward or backward as the path length or phase difference of the beam changes, indicating changes in distance or phase.
Fringe analysis	Analyzed to determine the magnitude and direction of rotation, useful in applications like fiber-optic gyroscopes.	Analyzed to measure changes in distance, wavelength, or phase shifts, suitable for precision measurements in scientific experiments.
Sensitivity	Highly sensitive to rotational changes, making it suitable for detecting angular velocity.	Sensitive to small path length differences, ideal for high-precision measurements of distance and refractive index.
Application areas	Widely used in navigation, geophysics, and rotation sensing.	Applied in fields like metrology, spectroscopy, and materials science for measuring small displacements and phase shifts.

The results highlight the distinct characteristics of the Michelson and Sagnac interferometers. The Michelson interferometer is suitable for precise measurements where uniformity and consistency of fringe patterns are crucial. Its ability to produce precise and uniform circular fringes makes it ideal for applications requiring high precision and stability (Shaddock et al., 1998). In contrast, the Sagnac interferometer, with its higher frequency

circular fringes, demonstrates superior sensitivity to rotational motion and environmental disturbances. This makes it highly suitable for applications in navigation and geophysics, where detecting small angular changes is essential (Usman et al., 2024; Ferrari et al., 2002). The comparative analysis reveals that while both interferometers can be used for similar applications, their optimal use cases differ significantly. The Michelson interferometer's stability and precision make it ideal for laboratory measurements, whereas the Sagnac interferometer's robustness against noise and environmental factors lends it to field applications (Malacara & Harris, 1970; Usman et al., 2021).

These findings have significant implications for the selection of interferometers in various scientific and industrial applications. The ability to choose the appropriate interferometer based on the specific requirements of the experiment or application can lead to more accurate and reliable measurements (Yu et al., 2024; Schnars & Jueptner, 2005).

4. Conclusions

In this study, we compared the performance and applications of the Michelson and Sagnac interferometers by capturing and analyzing interference patterns from alphabet character and fingerprint samples. Our findings highlight several vital differences and implications:

Alphabet character samples:

- The Michelson interferometer consistently produced circular fringes, demonstrating its reliable ability to measure small distances and refractive indices with high precision.
- The Sagnac interferometer, however, generated higher frequency circular fringes, showing its capability to produce distinct interference patterns due to its unique optical configuration.

Fingerprint samples:

- The Michelson interferometer produced concentric circular fringes, which aligns with its design and traditional applications in precise measurements.
- The Sagnac interferometer created linear fringes, indicating its sensitivity to rotational motion and potential for dynamic applications.

The results of this study provide valuable insights into the specific applications of both interferometers. With its straightforward setup and precise measurements, the Michelson interferometer is suitable for applications requiring high accuracy in measuring small distances and refractive indices. On the other hand, the Sagnac interferometer's ability to detect rotational motion and produce varied fringe patterns makes it ideal for navigation, geophysics, and dynamic studies applications.

Future research can build on these findings by further exploring additional sample types and configurations to understand the capabilities and limitations of both interferometers. Additionally, integrating advanced optical components and techniques could enhance the performance and expand the application range of these interferometers in scientific and industrial fields.

5. Acknowledgements

The authors would like to express their gratitude to the School of Science, King Mongkut's Institute of Technology Ladkrabang, for their generous support and encouragement throughout the course of this research. This support was instrumental in enabling the completion of this study.

6. Conflicts of Interest

The authors declare no conflict of interest with respect to the research, authorships, and/or publication of this article.

ORCID

Witoon Yindeesuk  <https://orcid.org/0000-0002-0674-8576>

Prathan Buranasiri  <https://orcid.org/0000-0001-7071-3194>

References

- Ferrari, J. A., Garbusi, E., & Frins, E. M. (2002). Modified Michelson interferometer with electrooptic phase control. *Optics Communications*, 209(4-6), 245-253. [https://doi.org/10.1016/s0030-4018\(02\)01730-3](https://doi.org/10.1016/s0030-4018(02)01730-3)
- Joenathan, C., Naderishahab, T., Bernal, A., Krovetz, A. B., Kumar, V. C. P., & Ganesan, A. R. (2017). Nanoscale tilt measurement using a cyclic interferometer with polarization phase stepping and multiple reflections. *Applied Optics*, 57(7), B52-B58. <https://doi.org/10.1364/ao.57.000B52>
- Malacara, D., & Harris, O. (1970). Interferometric measurement of angles. *Applied Optics*, 9(7), 1630-1633. <https://doi.org/10.1364/ao.9.001630>
- Schnars, U., & Jueptner, W. (2005). *Digital holography*. Springer eBooks. <https://doi.org/10.1007/b138284>
- Shaddock, D. A., Gray, M. B., & McClelland, D. E. (1998). Experimental demonstration of resonant sideband extraction in a Sagnac interferometer. *Applied Optics*, 37(34), 7995-8001. <https://doi.org/10.1364/ao.37.007995>
- Usman, A., Bhatranand, A., Jiraraksopakun, Y., Kaewon, R., & Pawong, C. (2021). Real-time double-layer thin film thickness measurements using modified Sagnac interferometer with polarization phase shifting approach. *Photonics*, 8(12), Article 529. <https://doi.org/10.3390/photonics8120529>
- Usman, A., Jiraraksopakun, Y., Kaewon, R., Pawong, C., & Bhatranand, A. (2022). The comparison of multi-stepping algorithms for real-time thickness measurement of transparent thin films using polarization settings. *Laser Physics*, 32(12), Article 125401. <https://doi.org/10.1088/1555-6611/aca026>
- Usman, A., Muhammad, K. S., Jiraraksopakun, Y., & Bhatranand, A. (2024). Comparative studies of circularly polarized light with phase shift in Sagnac and Mach-Zehnder interferometers. *Russian Physics Journal*, 67(3), 346-353. <https://doi.org/10.1007/s11182-024-03129-w>
- Xiao, S., Zhang, L., Wei, D., Liu, F., Zhang, Y., & Xiao, M. (2018). Orbital angular momentum-enhanced measurement of rotation vibration using a Sagnac interferometer. *Optics Express*, 26(2), 1997-2005. <https://doi.org/10.1364/oe.26.001997>
- Yu, W., Jiang, L., Zeng, K., Jing, X., & Jiang, Y. (2024). Michelson interferometer with Bessel beams. *Optics and Lasers in Engineering*, 177, Article 108146. <https://doi.org/10.1016/j.optlaseng.2024.108146>